JOURNAL OF GEOPHYSICAL RESEARCH, VOL. 107, NO. A7, 1149, 10.1029/2001JA000123, 2002

Ring current intensity estimated from low-altitude proton observations

F. Søraas, K. Aarsnes, and K. Oksavik
Department of Physics, University of Bergen, Bergen, Norway

D. S. Evans
NOAA Space Environment Center, Boulder, Colorado, USA

Received 3 May 2001; revised 6 November 2001; accepted 27 November 2001; published 31 July 2002.

[1] Using data from the low-altitude polar orbiting satellite NOAA-15 the proton precipitation rate into the upper atmosphere can be monitored with a 100-min time resolution. From the total power of precipitating protons in the midnight/evening local time sector, a parameter $Q(t)$ is used as a proxy for estimating the energy injection rate into the ring current (RC) due to energetic protons. The injection rate $Q(t)$ is not based upon solar wind parameters but directly on the observed proton precipitation rate. This is done under the assumption that the loss cone acts as a "splash catcher" for the protons injected into the RC. The protons in the loss cone thus do not represent a loss from the RC but are, in fact, a measure of the proton injection rate into the RC. Using the Burton equation and $Q(t)$ as a measure for the true energy injection rate, a value proportional to the energy content in the RC due to energetic protons can be calculated. Assuming a decay constant for the ions in the RC and that the magnetic field depression is proportional to the RC energy content, a RC index can be determined. When *Dst* is corrected for magnetopause and tail currents, the linear correlation coefficient between the corrected *Dst** and the RC index is between 0.8 and 0.9; thus $\sim$70–80% of the variance in this corrected *Dst** can be accounted for. The high correlation strongly indicates that $Q(t)$ is a measure of the true energy injection rate and that *Dst** is a measure of the energy content in the RC. Observations of proton precipitation measured by low-altitude polar-orbiting satellites thus have the potential for deriving a space-based *Dst* index in near real time that is not influenced by magnetic fields generated by magnetopause, field-aligned, and tail currents. *INDEX TERMS:* 2778 Magnetospheric Physics: Ring current; 2716 Magnetospheric Physics: Energetic particles, precipitating; *KEYWORDS:* Ring current, Dst, proton precipitation

1. Introduction

[2] The main physical cause for the ground-based magnetic perturbations at low latitude, represented by the *Dst* index, is the variability of the ring current (RC) composed of energetic ions encircling the Earth at altitudes of several Earth radii. The most widely used index of low-latitude activity is the hourly *Dst* index. It is the magnitude of the normalized horizontal component of the magnetic field as determined from the data obtained by four low-latitude observatories distributed in longitude. The derivation of the index is described by *Sugiura* [1964].

[3] There have been many suggestions on how the RC particles are injected into the magnetosphere. Are they injected by successive substorm expansions? Is the collapse of the tail-like field to a more dipolar configuration during the expansion phase the basic mechanism for this process, or are the injection caused by the global convection driven by dayside reconnection, as suggested by *McPherron* [1997]?

[4] In general, it is believed that enhanced convection transports RC particles to the inner magnetosphere during storms. The energetic particles in the RC, however, cannot account for all the variation in the *Dst*. The *Dst* is also influenced by magnetic fields generated by magnetopause, field-aligned, and tail currents. *McPherron* [1997] gives a comprehensive review of the different current systems that are contributing to the *Dst* in addition to the RC particles.

[5] When energetic protons are injected from the plasma sheet into the RC, a number of processes will lead to their precipitation into the atmosphere [*Lyons et al.*, 1999]. During their injection they are subjected to intense pitch angle scattering in the tail curved magnetic fields [*Sergeev et al.*, 1983]. This scattering is most intense in the midnight/evening sector. The intensity of these precipitating protons can thus serve as a measure for the RC energy injection rate.

[6] On statistical terms it has been established that there is a close association between the auroral indices and *Dst*. *Davis and Parthasarathy* [1967] found that the instanta-

0148-0227/02/2001JA000123$09.00

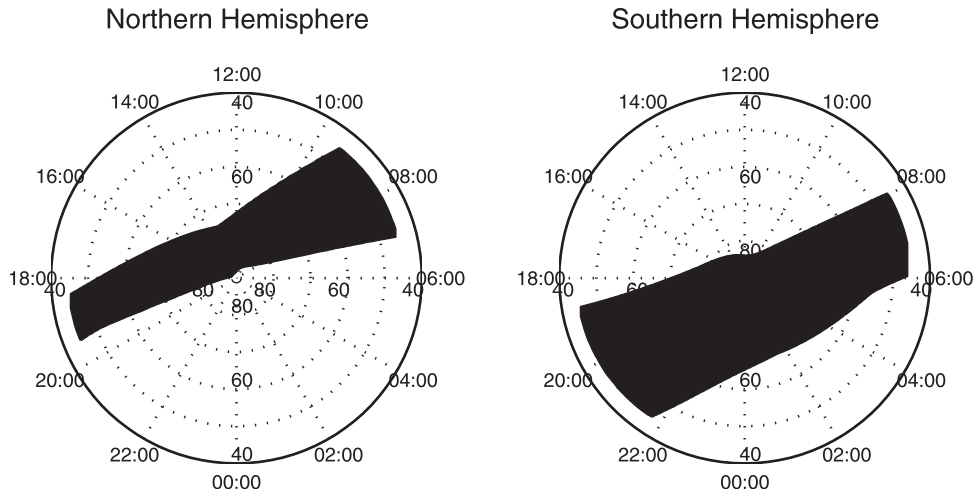

Figure 1. The invariant latitute (ILAT) magnetic local time (MLT) coverage of NOAA-15 during 1999.

neous *Dst* index could be well approximated by the linear superposition of the preceding 10 hours of the *AE* index. *Kamide and Fukushima* [1972] subsequently investigated this relation in greater detail. They concluded that *Dst* could be predicted by integrating the injection rate, e.g., rate at which energy is injected into the RC. To model the injection rate, they used the instantaneous *AE* index weighted by an assumed exponential particle decay rate. More recently, *Cade et al.* [1995] demonstrated that the *Dst* is linearly proportional to a recursively filtered *AL* index. Thus, using filters with the auroral indices as input the *Dst* could be fairly well approximated. This line of approach, however, did not link the injection rate to a specific physical mechanism but merely relied on the fact that the driving indices (*AE*, *AL*, or *Dst*) were all measures of geomagnetic activity reflecting, in turn, conditions in the solar wind (SW).

[7] In a study of the long time variations of protons in the radiation belt, *Søraas and Davis* [1968] noticed that the hundred to a few hundred keV protons were enhanced during storms. Depending on the size of the storm, this enhancement could occur all the way to $L = 2.5$. They further noticed that many fluctuations of trapped particle intensities were clearly caused by global changes in the Earth's magnetic field, and they used the trapped particle measurements themselves to compute the variations of the magnetic field. Søraas and Davis assumed that protons above 100 keV energy responded adiabatically to variations in the magnetic field and calculated the magnetic field radial distribution required to transform the observed radial distribution of proton intensity into a reference (quiet time) distribution. The correlation between the field required to transform the proton observations into the reference distribution, as determined by a least squares fit, and the observed *Dst* was around 0.8.

[8] *Burton et al.* [1975] were the first to attempt to predict the *Dst* index from solar wind conditions. From the solar wind parameters they estimated the RC injection rate. They could then calculate the RC part of the *Dst* using a reasonable charge exchange time constant to model the RC loss. This Burton et al. model has been subjected to several criticisms, and a comprehensive review of past work on this problem is given by *Feldstein* [1992].

[9] There has been much recent work on predicting the *Dst* index from upstream solar wind monitors. *O'Brien and McPherron* [2000] discuss a number of these new predictor methods and their relative accuracy. The implementation described provides a forecast time of ~1 hour.

[10] Instead of using an energy injection rate depending on SW parameters and auroral indices, the present study used an injection rate inferred from the measured intensity of protons appearing in the loss cone. The RC buildup and decay through the year 1999 have been analyzed using observations of protons measured by the NOAA-15 satellite. Protons/ions are the primary carriers of enhanced RC during magnetic storms, as their energy content dominates over the electrons.

2. Instrumentation

[11] The present study examined observations of protons from the Medium Energy Proton and Electron Detector (MEPED) on board the NOAA-15 satellite. The orbit of NOAA-15 is Sun-synchronous circular at an altitude of ~850 km. The NOAA-15 orbit plane is in the local evening/morning sector. A sketch of the magnetic local time/invarient magnetic latitude (MLT/ILAT) of the NOAA-15 footprint during 1999 is shown in Figure 1. Notice that the highest ILAT reached by the satellite in the Southern hemisphere sector varies between 65° and 90° during the day.

[12] While Figure 2 shows, for illustrative purposes, typical storm time proton observations from a NOAA-12 transit though the outer radiation belts, the detailed analysis presented here concentrated upon data from NOAA-15 because the solid-state detectors on board NOAA-12 had suffered significant radiation damage after >6 years in orbit. The MEPED instrument on NOAA-15 (which is similar to the one on NOAA-12) measures protons at angles of 10° and 80° to the local vertical. Observations from three differential energy channels, 30–80, 80–250, and 250–800 keV at each of those angles were used in this study.

[13] The instrument is sensitive to all energetic ions, but for purposes of this analysis it is assumed that the NOAA detector responses are only protons. A full description of the

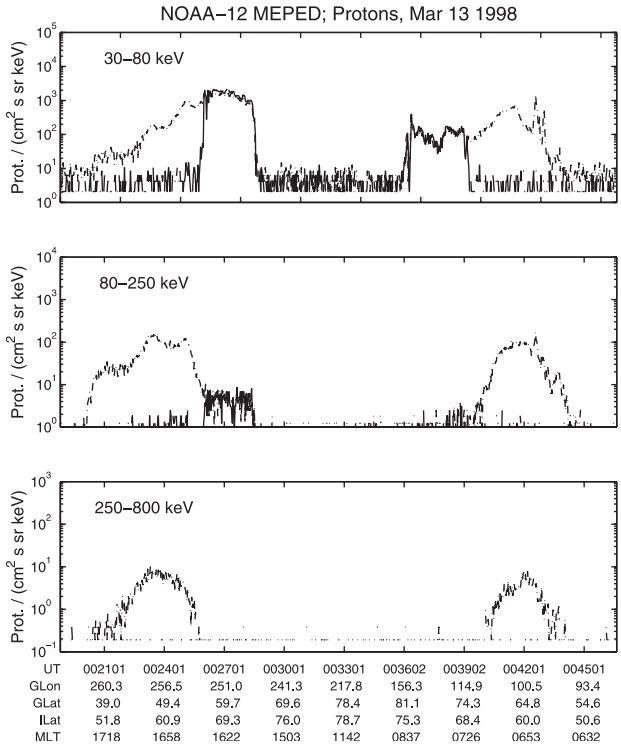

Figure 2. A typical NOAA pass. Protons with angles 10° and 80° with the vertical are measured in three energy channels ranging from 30 to 800 keV. The intensity of the 80° protons is shown by a dotted line, and the intensity of the 10° protons is shown by a solid line.

NOAA-15 satellite and the MEPED instrument is given by *Evans and Greer* [2000].

3. Observations

[14] Figure 2 shows data from a typical NOAA satellite pass traversing the mid- to high-latitude region in the Northern Hemisphere during the recovery phase of a storm taking place in March 1998. Protons with angles 10° and 80° with the local vertical are each measured in three energy channels 30–80, 80–250, and 250–800 keV. These channels cover the main RC energies responsible for the magnetic field depression at low latitudes. *Williams* [1981] states that ions in this energy range account for 70–80% of the energy density in the RC. The detector having an angle of 10° with the local vertical measures well inside the loss cone and the 80° one measures at the edge of the loss cone above ILAT equal to 50°.

[15] Both the 10° and 80° protons have a well-defined poleward boundary. The particle intensities drop 2 orders of magnitude when the satellite enters the polar cap. On the equatorward side the 10° protons exhibit a clear boundary. The intensity of the 80° protons, however, decreases gradually and does not exhibit a clear equatorward boundary. The region where the intensity at 10° and 80° protons is about equal is well defined and reveals the isotropic precipitation zone. This zone is very dynamic both in intensity and in latitudinal extent. The equatorward border of this zone is called the isotropic boundary (IB). Protons in the isotropic zone are subjected to intense pitch angle scattering, and the ones inside the loss cone will penetrate into the atmosphere and get lost. For a discussion on energetic proton precipitation during geomagnetic storms, see *Hauge and Søraas* [1975].

[16] On the dawnside in Figure 2 a region of enhanced proton intensity at midlatitudes around ILAT 58° and 0650 MLT can be seen. Such enhanced regions of anisotropic pitch angle distributions are most likely due to protons scattered by resonant wave-particle interaction at or near the plasmapause, as discussed by *Søraas et al.* [1999] and *Yahnina et al.* [2000] and represent a loss of RC particles in the recovery phase of a geomagnetic storm.

[17] Figure 3 shows the intensity (color-coded) of protons precipitating into the evening local time sector on an orbit by orbit basis during the second half of 1999. The measured proton intensities in each NOAA-15 pass are plotted versus ILAT and time. Figures 3a–3c show precipitating protons in the energy channels 30–80, 80–250, and 250–800 keV. Figures 3d–3f show locally mirroring protons for similar energy channels, and Figure 3g shows the measured *Dst*. The Southern Hemisphere evening data are shown as the satellite here gives better MLT coverage than in the Northern Hemisphere as seen from Figure 1. The midnight/evening MLT sector is used as protons injected into the RC appear (pass through) in this MLT sector. Comparing the total precipitation in the evening sector with the one in the morning sector (see Figure 2) shows that precipitation is most intense in the evening sector.

[18] The last 6 months of 1999 exhibit one large (−225 nT on day 295) and two small (−160 and −90 nT on days 265 and 347) geomagnetic storms. A comparison of the intensity and latitudinal extent of the proton fluxes with *Dst* shows that every negative deviation in *Dst* is accompanied by an increase in proton precipitation and an equatorward movement of the precipitation zone. During each major enhancement in geomagnetic activity, there is increased proton precipitation and the proton injection extends to lower latitude and further into the inner magnetosphere. This can clearly be seen in the larger storms (days 265 and 295 of 1999), where the precipitation is more intense and penetrates deeper into the magnetosphere than during other times. As demonstrated during the relatively quiet days 182–202, the *Dst* is sensitive to the proton injection, as even small increases in the proton precipitation rate shows up in the *Dst* index.

[19] Figure 4b gives the *Dst* during the main and early phases of the large October 22 storm. In the main phase of the storm (day 295 in Figure 3) the *Dst* index went down to −225 nT. In the recovery phase, *Dst* exhibited the typical two-phase recovery commonly observed in large storms, recovering first quickly during half a day from −225 to −75 nT and then more slowly from around −75 nT toward the quiet level. Figure 4a shows how the IB for the 30–80 keV protons changed through the storm. At the start of the storm the IB quickly went down to an ILAT of 54° and reaching down to 53° during the main phase of the storm. This deep penetration of the proton precipitation lasted during the main phase of the storm. Coincident with the fast recovery of the *Dst* the IB retreated to an ILAT of of around 62° in <8 hours. The

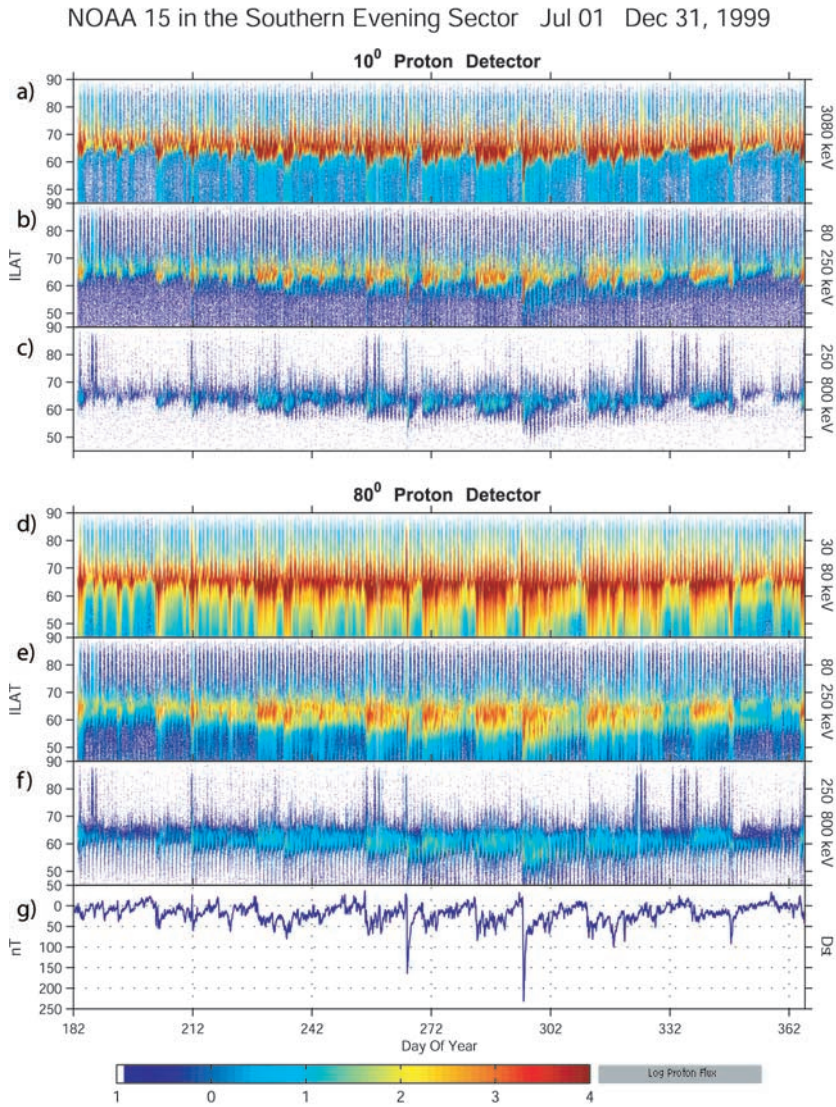

Figure 3. The precipitating proton flux (*protons/cm*^{2}*sr s keV*) into the evening local time sector during the six last months of 1999. Each NOAA-15 pass is plotted versus ILAT, and the observed proton flux is color-coded. (a–c) Precipitating protons in the energy channels 30–80, 80–250, and 250–800 keV. (d–f) Same information as in Figures 3a–3c, but for the mirroring protons. (g) Measured *Dst* during the period considered.

IB of the protons thus exhibits a leap in latitude at the end of the storm main phase, most likely connected with a reduction in the magnetospheric convection field.

[20] In Figure 3 it was seen that the proton intensity for both the 10° and 80° detectors exhibit a daily modulation, both at high ILAT (above 65°) and at low latitudes below the IB. In these regions the particle intensities exhibit a comb-like structure with a 1-day period. The high-latitude modulation is caused by the satellite orbit (see Figure 1) precluding on a daily basis some orbits sampling particles above 65° ILAT.

[21] The low-latitude modulation seen most clearly in the 80° detector that observes protons at near local mirroring pitch angles. This modulation reflects the well-known variation of trapped particle intensities with geographic longitude when observed at a constant low altitude that arises because of the longitudinal variation in Earth's magnetic field strength [*Berg and Søraas*, 1972].

4. Modeling the RC Energy Buildup and Decay

[22] *Dessler and Parker* [1959] and *Sckopke* [1966] derived a formula, which relates the total amount of energy in the RC to the magnetic perturbation at the Earth's center by

$$\frac{\Delta B}{B_s} = -\frac{2K}{3U_M},$$

where ΔB is the perturbation at the center of the Earth, B_s is the surface dipole strength at the equator, K is the total energy in the RC due to particles, and U_M is the total energy of the Earth's dipole field above the Earth's surface. Putting realistic

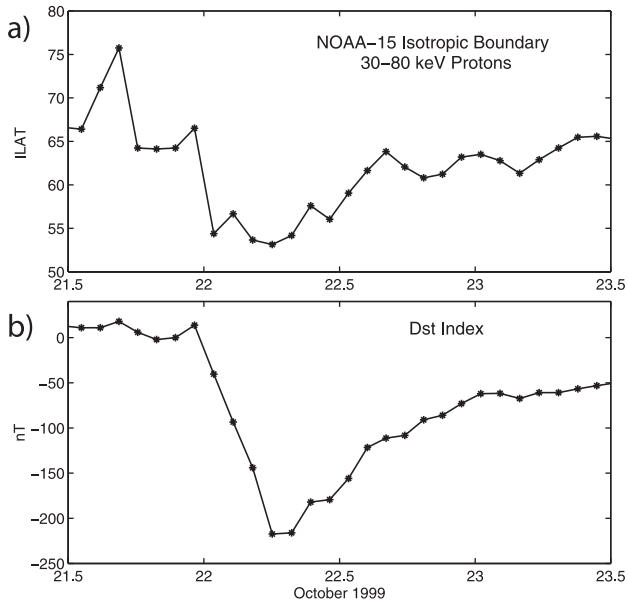

Figure 4. (a) How the IB (isotropic boundary) for the 30–80 keV protons changed during the October 1999 storm. (b) *Dst* through the storm.

values into this equation, one finds that an energy content of 4×10^{13} J into the RC corresponds to a 1-nT depression of the magnetic field at the Earth's equator [*Williams*, 1981].

[23] As already stated, the main magnetic field depression at low latitudes at the Earth's surface is caused by the RC. However, other magnetospheric current systems than the RC system can also cause field perturbations at the Earth's surface. For example, dayside magnetopause currents are known to contribute to the *Dst* index. It is, however, possible to correct for solar wind dynamic effects using a relationship suggested by *Burton et al.* [1975] and developed further by *Gonzalez et al.* [1989]

$$Dst^* = Dst - (0.02v\sqrt{n} - 20 \text{ nT}),$$

where v is the solar wind speed in km/s, n is the number density in particles per cubic centimeter, 20 nT is a correction factor related to the effect of magnetopause currents for average solar wind conditions, and *Dst** is the so-called pressure-corrected *Dst*.

[24] It has also been suggested that the nightside tail current sheet can significantly affect the *Dst* index during high magnetic activity periods when the currents are intense and flow relatively close to the Earth. *Turner et al.* [2000] have found that the tail current contribution to the *Dst* is proportional to the *Dst*. Using their Figure 5[6], the tail contribution to the *Dst* can be approximated by the formula

$$\Delta B_{\text{tail}} = 0.245 \times Dst + 5 \text{ nT}.$$

[25] These corrections have been applied to the *Dst* for 1999, and a new corrected version *Dst** has been calculated. The *Dst** should be a better approximation for the energy content in the RC than the measured *Dst*.

[26] From the Burton formula:

$$dK/dt = Q(t) - K/T,$$

the energy content K in the RC due to energetic particles can be estimated. $Q(t)$ is the RC energy injection rate and $T = 7.7$ hours is the RC decay constant.

[27] Several loss mechanisms like charge exchange, convection losses at the front of the magnetosphere, wave-

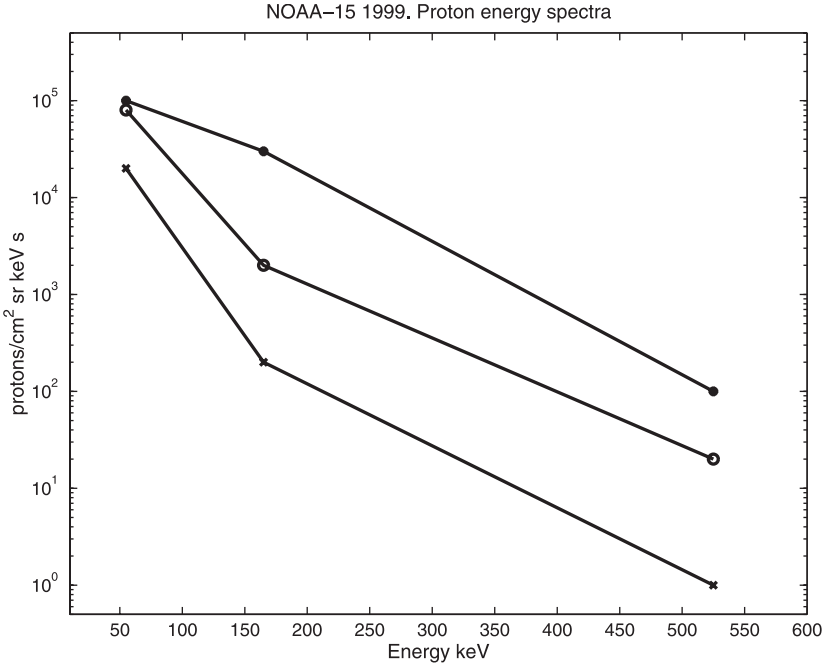

Figure 5. NOAA-15 MEPED proton spectra for 19 February (line with stars), 22 October (line with circles), and 23 November (line with crosses) 1999.

particle interaction, etc., are lumped into the decay constant *T*. The mechanisms for the decay of the storm time RC are still a matter of debate. *Jordanova et al.* [1996] have shown that charge exchange is the most important collisional loss mechanism. *Kozyra et al.* [1998] found that in addition to charge exchange loss, convection loss through the dayside magnetopause, and Coulomb collision loss, other loss processes such as wave-particle interactions must be operating. *Liemohn et al.* [1999] demonstrated that the convective loss through the dayside magnetopause is dominant in the main phase of a magnetic storm.

[28] In the RC, H^+ is the dominant ion species, with the O^+ contribution increasing during active times. During intense storms (such as the one on 22 October in Figure 3), O^+ is the dominant ion species during the storm main phase, contributing 50–80% of the total energy density of the RC depending on the size of the storm [*Daglis et al.*, 1999]. Energetic O^+ enhancements are usually short-lived [*Daglis et al.*, 1996] but can remain above 30% for more than 24 hours [*Daglis et al.*, 1993].

[29] In our study the total energy input to the RC is calculated assuming that all ions are H^+. As known, this is not the case during active times, and the error introduced in our calculations by the all proton assumption will now be discussed.

[30] The MEPED solid-state detectors will also respond to He^+ and O^+. The only difference between the way the detector will respond to those ions and to H^+ is the energy lost by the ion in passing through the 20 $\mu g/cm^2$ Al layer on the face of the detector and the detector dead layer. Combining energy loss curves given by *Northcliffe and Schilling* [1970] and semiempirical results for electronic stopping power by *Andersen and Ziegler* [1977] for various ions passing through different materials, the energy loss for hydrogen, helium, and oxygen at different energies in the dead layer of a solid-state detector has been calculated [*Johansen*, 1990; *Johansen et al.*, 1991]. A solid-state detector system with an electronic threshold of 190 keV would respond to 200 keV hydrogen, 215 keV helium, and 230 keV oxygen, and an electronic threshold of 23 keV would respond to 30 keV hydrogen, 30 keV helium, and 45 keV oxygen. This reflects the greater energy loss in the Al layer for oxygen than for lighter ions. In short, if the precipitating ions were O instead of H, the low-energy threshold for computing the energy fluxes would not be 30 keV but some higher value estimated to be 45 keV for oxygen.

[31] The energy limits of the three energy bands for the MEPED solid-state detectors would thus move toward higher energies for oxygen, and the three differential energy bands will be ~45–100, 100–280, and 280–850 keV for oxygen. This means that the energy flux assuming hydrogen would underestimate the oxygen energy fluxes as the characteristic energy in each channel is increased. Calculating the energy flux using the three energy spectra, shown in Figure 5 for 19 February, 22 October, and 23 November, will give an energy flux of 5.8, 1.4, and 0.31 $ergs/cm^2$ s, respectively, assuming hydrogen and 7.3, 1.9, and 0.44 $ergs/cm^2$ s assuming oxygen. This gives a worst-case error of around 30% well inside the other uncertainties contained in our estimate of the ion energy flux into the atmosphere. If, on the other hand, we had estimated particle energy density, an assumption of H instead of O would make a factor of 4 difference for the same particle energy.

5. The RC Injection

[32] *O'Brien* [1964] discussed two models to explain the precipitation of electrons at high latitudes: the leaky bucket and the splash catcher models. From his Injun 1 studies, *O'Brien* [1964, p. 14] suggested "that precipitation occurs principally during the acceleration process and that the precipitating particles are fresh particles." He then further states "The outer zone should then be regarded not as a 'leaky bucket' that occasionally spills out particles to cause auroras but rather as a bucket that catches a little of the splash from the acceleration mechanism. For want of a better phrase, it is a splash-catcher." O'Brien states that a test of the splash catcher model is simply to determine whether the flux of trapped electrons increases when electrons are precipitated.

[33] As discussed in section 3, the *Dst* is closely connected with the observed proton precipitation. *Dst* experiences a decrease (indicating an increase in the RC energy) when the proton precipitation flux increases. The proton precipitation does behave in accordance with the splash catcher model. What we observe at low altitudes in the premidnight sector is not a loss of particles from the RC but a splash of particles into the loss cone. This occur when the RC experiences an injection of fresh particles from the plasma sheet. In our analysis we assume that there is proportionality between the splash and what is injected into the RC.

[34] From observations at low altitudes the total injection rate into the RC can not be calculated. We can, however, calculate the total power $Q^*(t)$ of precipitating protons into the evening quadrant (1800–2400 MLT sector). This splash is taken as a measure of the RC energy injection rate. It is, however, important to notice that we are making an estimate of energy injection from an estimate of precipitating energy, not a calculation of particle energy density.

[35] From the NOAA data the power due to protons in the energy range 30–800 keV through a horizontal area of 1 cm^2 along the ILAT trajectory of the satellite is determined. Each power value is weighed by a factor taking into account the area of a quart of a circle with radius R_E cos (ILAT) and a width of 1 cm, which gives more weight to protons penetrating closer to the Earth. R_E is the radius of the Earth. All the values are then summed over ILAT to give $Q^*(t)$ the total precipitating power in the premidnight quadrant. This calculation is based on the assumption that one pass through the evening MLT sector is representative for the whole evening quadrant. The time resolution of the measurements is around 100 min, that is, one sample per orbit.

6. Results

[36] Figure 6a shows the total power $Q^*(t)$ during the days 220–360 of 1999 based on the NOAA-15 proton measurements shown in Figure 3. The energy input ranges from 0.5 to >50 GW, that is, a variation by a factor of more than a hundred depending on geomagnetic activity. In Figure 6e the measured *Dst* is shown, and Figure 6d displays the corrected *Dst**. It is seen that for every increase

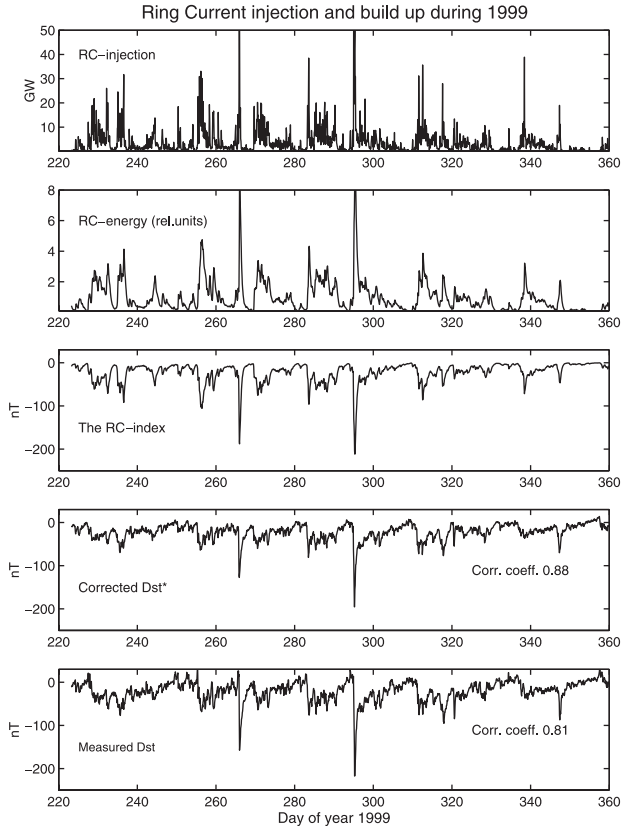

Figure 6. (a) Total power Q^* (t) of protons into the upper atmosphere in the premidnight local time sector during the last 6 months of 1999. (b) "RC energy" as calculated from the Burton relation using Q^* (t) as the injection rate. (c) RC index normalized to the *Dst** index shown in Figure 6d. (e) Measured *Dst* index.

in Q^* (t) the *Dst* index goes negative, indicating that the energy content in the RC increases in accordance with the splash catcher model.

[37] In Figure 6b the "RC energy" content has been calculated from the Burton equation with Q^* (t) as the injection rate. The RC energy content is proportional to the magnetic field depression and can thus be converted to an index. This index is now normalized (scaled by a factor) to have the same average value as the corrected *Dst**, and we obtain an RC index, a space-based version of *Dst** shown in Figure 6c.

[38] The overall agreement between the RC index and the pressure-corrected *Dst** is good. The two parameters track each other very well with a linear correlation coefficient of 0.88 for the whole period considered. The correlation with the measured *Dst* is somewhat lower (0.81). This is in accordance with our model since the *Dst** is a more direct measurement of the RC energy than the *Dst*.

[39] In Figure 7 the RC injection Q^* (t), the RC index (dotted line), and the corrected *Dst** (solid line) for the whole of 1999 are shown. Data for each quarter of the year are shown separately, and it is seen that the RC index and *Dst** track each other well during the whole year of 1999. The correlation coefficient for each quarter of the year is 0.89, 0.85, 0.86, and 0.89.

[40] According to *McPherron* [1997] the *Dst* has an accumulated error of the order 10–30 nT, which appear as random noise in the data. If normally distributed noise with a standard deviation of 10 nT is added to the RC index and a correlation with the unmodified RC index is performed, the correlation is 0.90. This further shows that a correlation coefficient above 0.8 between the RC index and the corrected *Dst** is highly significant.

[41] As stated, the RC index and the *Dst** track each other well; however, there are some cases (days 50, 211, and 257) where they deviate largely. The most pronounced discrepancy between the *Dst** and the RC index, as shown in Figure 7, occurs on day 50.55 (19 February 1315 UT, 1945 MLT) that is in the recovery phase of a −120 nT storm. The reason for this difference between the calculated RC index and the corrected *Dst** is not known. On this occasion, however, the NOAA-15 protons exhibit an unusually hard spectrum with a power input of (5.8 ergs/cm^2 s) above 30 keV. In Figure 5 this spectrum is compared with spectra from the 22 October storm and on 23 November referring to quiet geomagnetic conditions. As seen, there is a large difference between the spectra, in particular for energies above a hundred keV. On 19 February, ~75% of the energy content was at energies above 80 keV, while on 22 October and 23 November only 20% and 10%, respec-

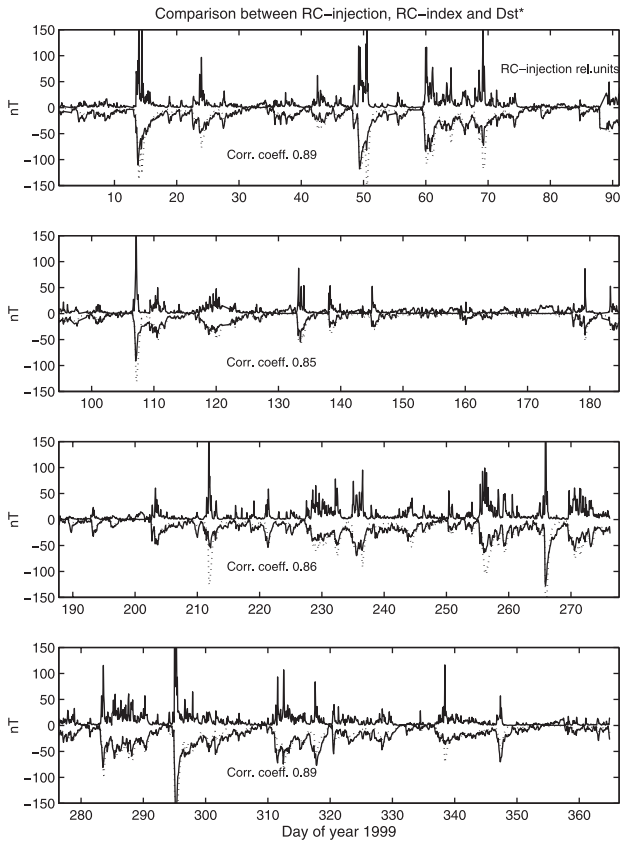

Figure 7. A comparison between the RC injection rate (relative scale), the RC index (dotted line), and the corrected *Dst** (solid line) for the year 1999. Each quarter of the year is considered separately, and the correlation coefficient between the RC index and *Dst** index is computed.

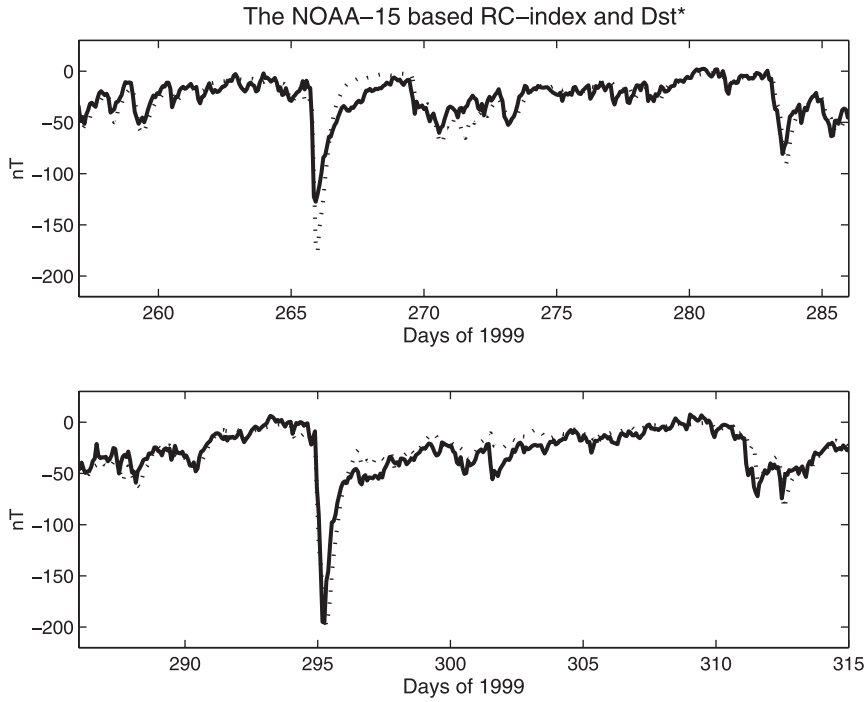

Figure 8. A comparison between the RC index (dotted line) and the corrected *Dst** index (solid line) for days 257–315 of 1999.

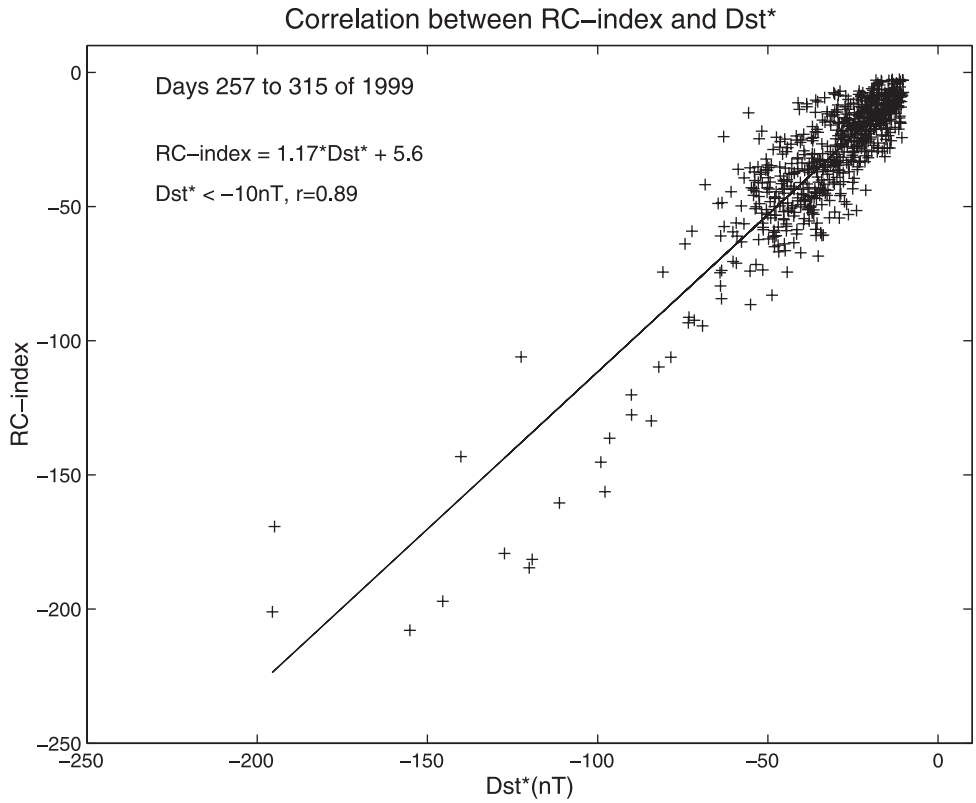

Figure 9. The RC index plotted versus the corrected *Dst** index for days 257–315 of 1999. The linear fit and the correlation coefficient between the two parameters are shown.

tively, were above this energy. A possible explanation for the large difference between the RC index and the *Dst** on 19 February could be that the high-energy ions will rapidly transit through the magnetosphere on open drift paths that intersect the dayside magnetopause. As high-energy ions do not convect as close to the Earth as the lower-energy ions do, they will complete a smaller segment around the Earth, and consequently, their contribution to the *Dst* will be reduced.

[42] In order to show the correlation between the RC index and *Dst** in more detail the two parameters for days 257 to 315 of 1999 are plotted in Figure 8. This time period covers the two geomagnetic storms on days 265 and 295 and intervals between the storms with quiet geomagnetic conditions. It is seen that the two parameters track each other quite well, both during the storms and during the more quiet times. A scatterplot of the RC index and *Dst** for the period presented in Figure 8 is shown in Figure 9. Positive values of *Dst** are excluded in the scatterplot as the RC index by nature only can attain negative values, as the energy in the RC can not be negative. The relationship between the two parameters is fairly linear, but as most of the points in the plot have *Dst** values above −60 nT, the overall linear fit is biased toward quiet geomagnetic conditions. The fit is shown by a solid line in Figure 9. This indicates that the injection rate $Q^*(t)$ is proportional to the RC energy injection rate. The overall linear correlation coefficient between the two parameters for the time period shown in Figure 8 is 0.89.

7. Conclusions

[43] The isotropic proton precipitation in the premidnight sector is a good measure for the RC energy injection rate. When the RC index is normalized, i.e., is multiplied by a factor, it tracks the corrected *Dst** very well, and ∼70–80% of the variance in the *Dst** can be accounted for by our RC index.

[44] *Dst** can thus to some degree be estimated from the measured proton precipitation. The correlation between the two quantities is high, indicating that the RC is fed by protons being injected from the plasma sheet. It further shows that the corrected *Dst** is a good measure of the particle energy content in the RC. The absolute energy content in the RC, however, cannot be calculated by our method. Because of the good correlation between the RC index and the measured *Dst* it would be possible to use observations from the NOAA satellites to derive a space-based equivalent of the *Dst* index in near real time.

[45] We are of the opinion that the RC index based on the ''estimated'' proton injection rate, derived from the true proton precipitation power, gives a good picture of the true RC, as it is not influenced by other current systems in the magnetosphere. The injection rate is an estimate based upon a direct measure of ion precipitation rate and not upon solar wind or auroral parameters.

[46] **Acknowledgments.** We thank Dag Vartdal Carlsen for calculating the isotropic boundary and the two referees for valuable comments. We would like to thank the Norwegian Research Council for financial support.

[47] Janet G. Luhmann thanks Ioannis Daglis and another referee for their assistance in evaluating this paper.

References

Andersen, H. H., and J. F. Ziegler, *The Stopping and Ranges of Ions in Matter*, vol. 3, *Hydrogen: Stopping Powers and Ranges in All Elements*, Pergamon, New York, 1977.

Berg, L. E., and F. Søraas, Observations suggesting weak pitch angle diffusion of protons, *J. Geophys. Res.*, *77*, 34, 1972.

Burton, R. K., R. L. McPherron, and C. T. Russell, An empirical relationship between interplanetary conditions and *Dst*, *J. Geophys. Res.*, *80*, 4204, 1975.

Cade, W. B., III, J. J. Sojka, and L. Zhu, A correlative comparison of the ring current and auroral electrojets using geomagnetic indices, *J. Geophys. Res.*, *100*, 97, 1995.

Daglis, I. A., E. T. Sarris, and B. Wilken, AMPTE/CCECHEM observations of the ion population at geosynchronous altitudes, *Ann. Geophys.*, *11*, 685, 1993.

Daglis, I. A., W. I. Axford, S. Livi, B. Wilken, M. Grande, and F. Søraas, Auroral ionospheric ion feeding of the inner plasma sheet during substorms, *J. Geomagn. Geoelectr.*, *48*, 729, 1996.

Daglis, I. A., R. M. Thorne, W. Baumjohann, and S. Orsini, The terrestrial ring current: Origin, formation and decay, *Rev. Geophys.*, *37*, 407, 1999.

Davis, T. N., and R. Parthasarathy, The relationship the polar magnetic activity DP and the growth of the geomagnetic ring current, *J. Geophys. Res.*, *72*, 5825, 1967.

Dessler, A. J., and E. N. Parker, Hydromagnetic theory of magnetic storms, *J. Geophys. Res.*, *64*, 2239, 1959.

Evans, D. S., and M. S. Greer, Polar orbiting environmental satellite space environment monitor, 2, Instrument descriptions and archive data documentation, *NOAA Tech. Memo. OAR SEC-93*, Natl. Oceanic and Atmos. Admin., Boulder, Colo., 2000.

Feldstein, Y. I., Modeling of the magnetic field of magnetospheric ring current as a function of interplanetary medium parameters, *Space Sci. Rev.*, *59*, 83, 1992.

Gonzalez, W. D., B. T. Tsurutani, A. L. C. Gonzalez, E. J. Smith, F. Tang, and S. I. Akasofu, Solar-wind magnetosphere coupling during intense magnetic storms (1978–1979), *J. Geophys. Res.*, *94*, 8835, 1989.

Hauge, R., and F. Søraas, Precipitation of >115 keV protons in the evening and forenoon sectors in relation to magnetic activity, *Planet. Space Sci.*, *23*, 1141, 1975.

Johansen, G. A., Development and analysis of silicon based detectors for low energy nuclear radiation, thesis, Dep. of Phys., Univ. of Bergen, Bergen, Norway, 1990.

Johansen, G. A., J. Stadsnes, F. Søraas, and T. E. Hansen, Detection of 10–20 keV H^+, He^+ ions and electrons by planar oxide passivated and ion implanted silicon diodes, *Nucl. Instrum. Methods Phys. Res., Sect. B*, *62*, 162, 1991.

Jordanova, V. K., L. M. Kistler, J. U. Kozyra, G. V. Khazanov, and A. F. Nagy, Collisional loss of ring current ions, *J. Geophys. Res.*, *101*, 111, 1996.

Kamide, Y., and N. Fukushima, Analysis of magnetic storms with DR-indices for equatorial ring current fields, *Rep. Ionos. Space Res. Jpn.*, *26*, 79, 1972.

Kozyra, J. U., M.-C. Fok, E. R. Sanchez, D. S. Evans, D. C. Hamilton, and A. F. Nagy, The role of precipitation loss in producing the rapid early recovery phase of the great magnetic storm of February 1986, *J. Geophys. Res.*, *103*, 6801, 1998.

Liemohn, M. W., J. U. Kozyra, V. K. Jordanova, G. V. Khazanov, M. F. Thomsen, and T. E. Cayton, Analysis of early phase ring current recovery mechanisms during geomagnetic storms, *Geophys. Res. Lett.*, *26*, 2845, 1999.

Lyons, L. R., H. E. J. Koskinen, J. B. Blake, A. Egeland, M. Hirahara, M. Øieroset, P. E. Sandholt, and K. Shiokawa, Processes leading to plasma losses into the high-latitude atmosphere, in *Magnetospheric Plasma Sources and Losses, Space Sci. Ser. Int. Space Sci. Inst.*, vol. 6, edited by B. Hultqvist, M. Øieroset, G. Paschmann, and R. Treumann, p. 85, Kluwer Acad., Norwell, Mass., 1999.

McPherron, R. L., The role of substorms in the generation of magnetic storms, in *Magnetic Storms, Geophys. Monogr. Ser.*, vol. 98, edited by B. T. Tsurutani et al., p. 131, AGU, Washington, D. C., 1997.

Northcliffe, L. C., and R. F. Schilling, Range and stopping-power tables for heavy ions, *Nucl. Data, Sect. A*, *7*(3–4), 233, 1970.

O'Brien, B. J., High-latitude geophysical studies with satellite Injun 3, 3, Precipitation of electrons into the atmosphere, *J. Geophys. Res.*, *69*, 13, 1964.

O'Brien, T. P., and R. L. McPherron, Forecasting the ring current index *Dst* in real time, *J. Atmos. Sol. Terr. Phys.*, *62*, 1295, 2000.

Sckopke, N., A general relation between the energy of trapped particles and the disturbance field near the Earth, *J. Geophys. Res.*, *71*, 3125, 1966.

Sergeev, V. A., E. M. Sazhina, N. A. Tsyganenko, J. Å. Lundblad, and F. Søraas, Pitch-angle scattering of energetic protons in the magnetotail current sheet as the dominant source of their isotropic precipitation into the nightside ionosphere, *Planet. Space Sci.*, *31*, 1147, 1983.

Søraas, F., and L. R. Davis, Temporal variations of 100 keV to 1700 keV trapped protons observed on satellite Explorer 26 during first half of 1965, *Rep. X-612-68-328*, Goddard Space Flight Cent., Greenbelt, Md., 1968.

Søraas, F., K. Aarsnes, J. Å. Lundblad, and D. S. Evans, Enhanched pitch angle scattering of protons at mid-latitudes during geomagnetic storms, *Phys. Chem. Earth, Part C*, *24*, 287, 1999.

Sugiura, M., Hourly values of equatorial *Dst* for the IGY, *Ann. Int. Geophys. Year*, *35*, 49, 1964.

Turner, N. E., D. N. Baker, T. I. Pulkkinen, and R. L. McPherron, Evaluation of tail current contribution to *Dst*, *J. Geophys. Res.*, *105*, 5431, 2000.

Williams, D. J., Ring current composition and sources: An update, *Planet. Space Sci.*, *29*, 1195, 1981.

Yahnina, T. A., A. G. Yahnin, J. Kangas, and J. Manninen, Proton precipitation related to Pc 1 pulsations, *Geophys. Res. Lett.*, *27*, 3575, 2000.

K. Aarsnes, K. Oksavik, and F. Søraas, Department of Physics, University of Bergen, Allégaten 55, N-5007 Bergen, Norway. (kjell.aarsnes@fi.uib.no; kjellmar.oksavik@fi.uib.no; finn.soraas@fi.uib.no)

D. S. Evans, NOAA Space Environment Center, 325 Broadway, Boulder, CO 80305, USA. (devans@sec.noaa.gov)